

Multiphysics Modeling and Understanding for Plasmonic Organic Solar Cells

*Wei E.I. Sha, Wallace C.H. Choy, and
Weng Cho Chew*

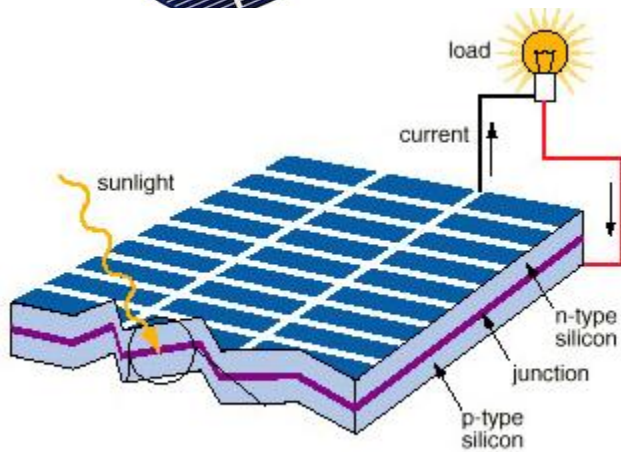
Department of Electrical and Electronic Engineering,
The University of Hong Kong, Hong Kong

Email: wsha@eee.hku.hk (W.E.I. Sha)

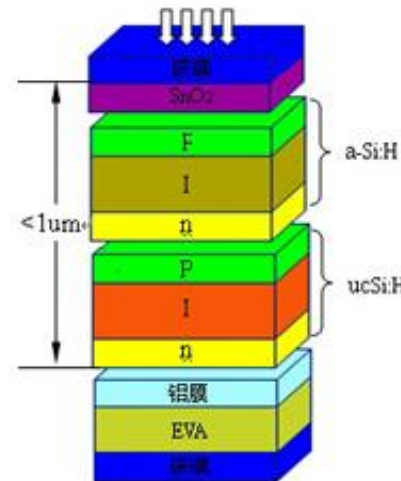


Organic Solar Cell (1)

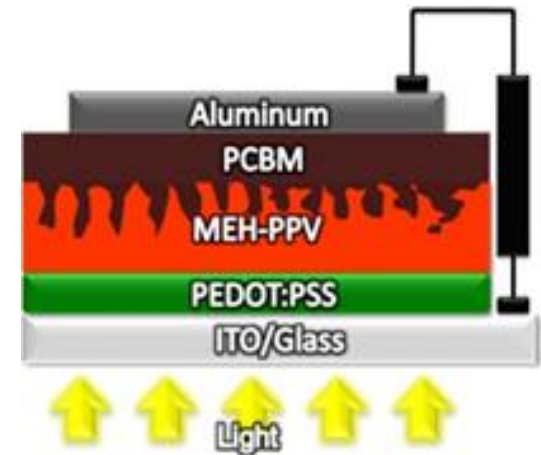
Advances of solar cell technology



monocrystalline silicon solar cell



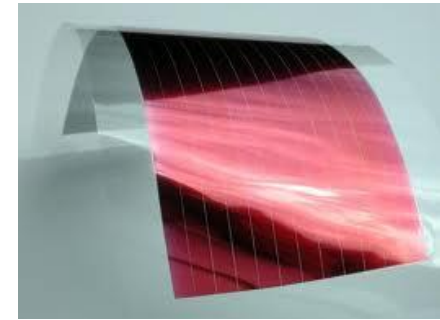
amorphous/polycrystalline silicon solar cell



organic solar cell

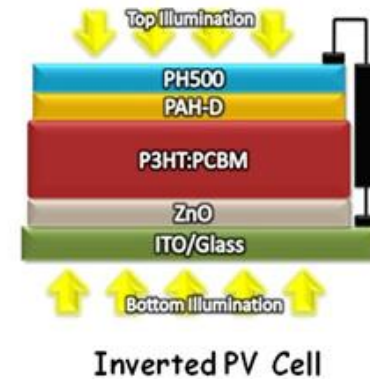
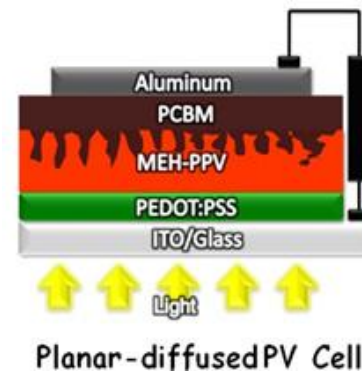
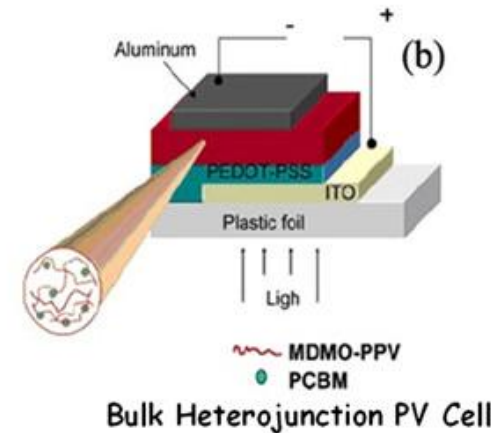
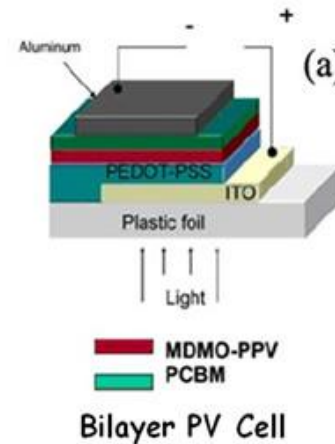


Organic Solar Cell (2)



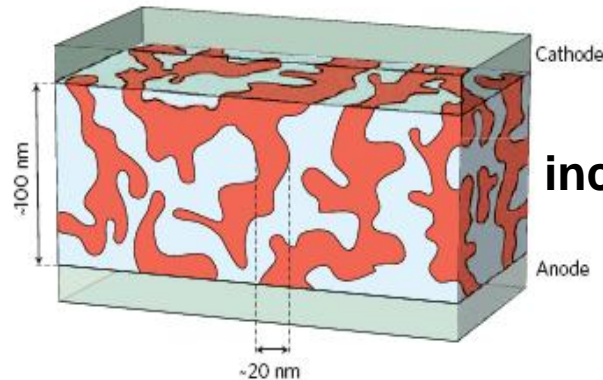
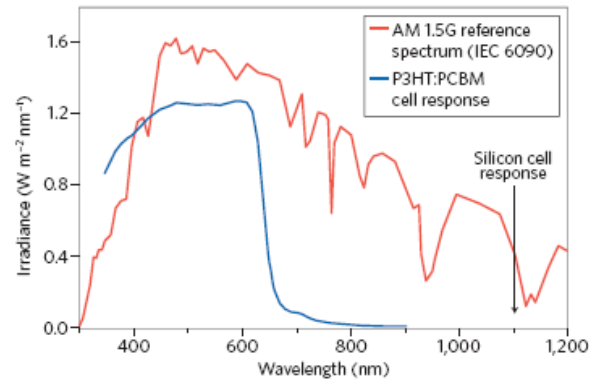
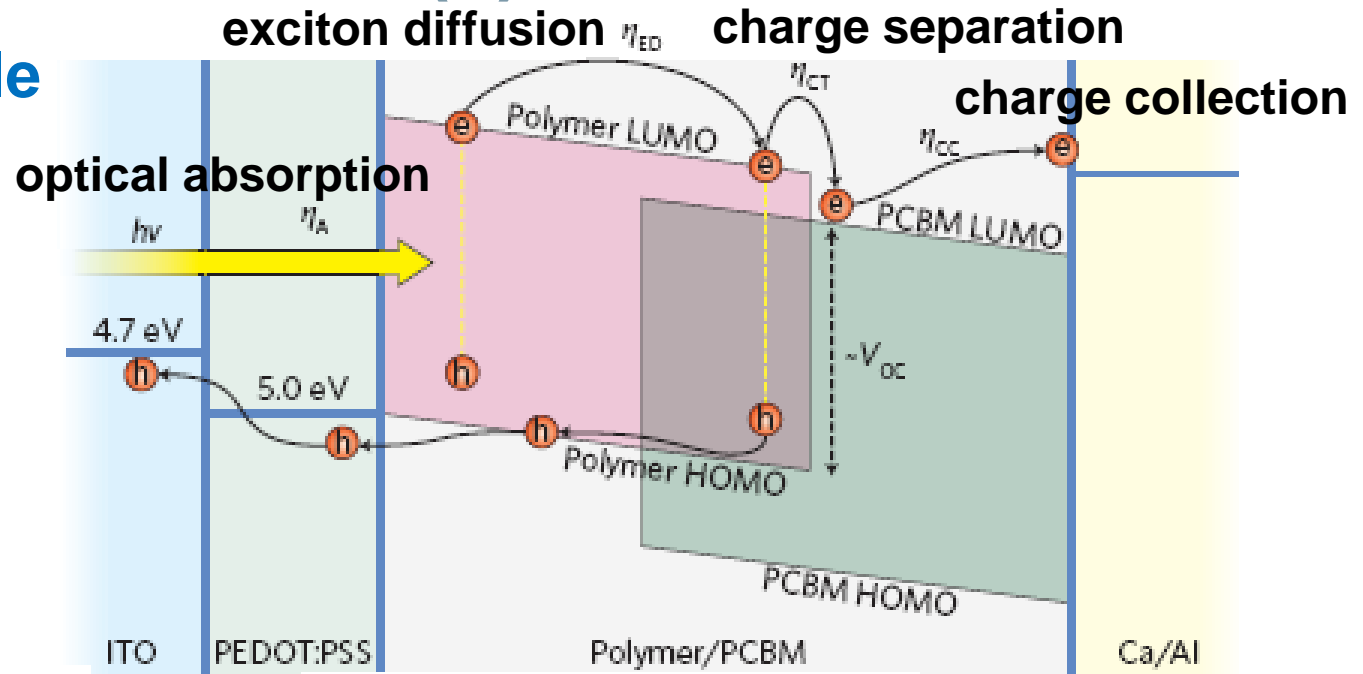
Thin-film organic solar cell

- ✓ *low-cost processing*
- ✓ *mechanically flexible*
- ✓ *large-area application*
- ✓ *environmentally friendly*
- X *low exciton diffusion length*
- X *low carrier mobility*



Organic Solar Cell (3)

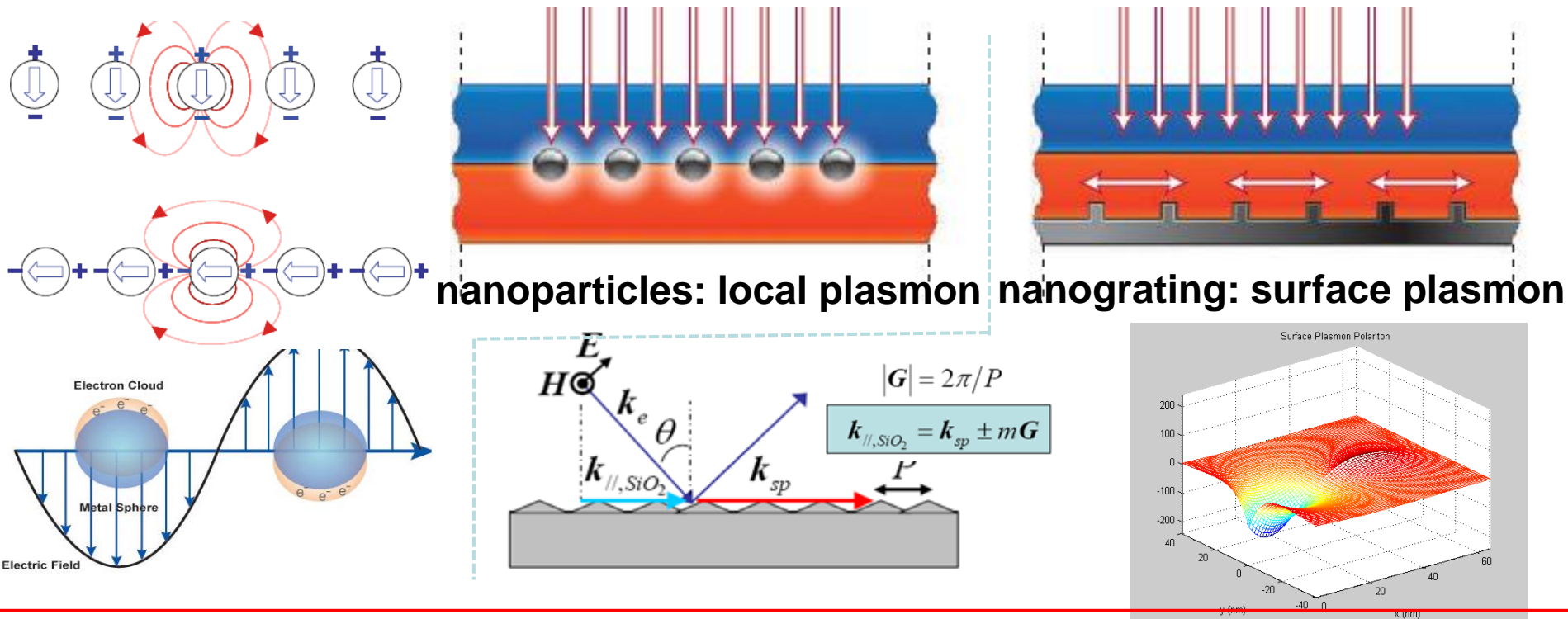
Working principle



Plasmonic Organic Solar Cell

Why optical enhancement?

The thickness of the active layer must be smaller than the exciton diffusion length to avoid bulk recombination. As a result, the thin-film organic solar cell has poor photon absorption or harvesting. Plasmonic solar cell is one of emerging solar cell technologies to enhance the optical absorption.

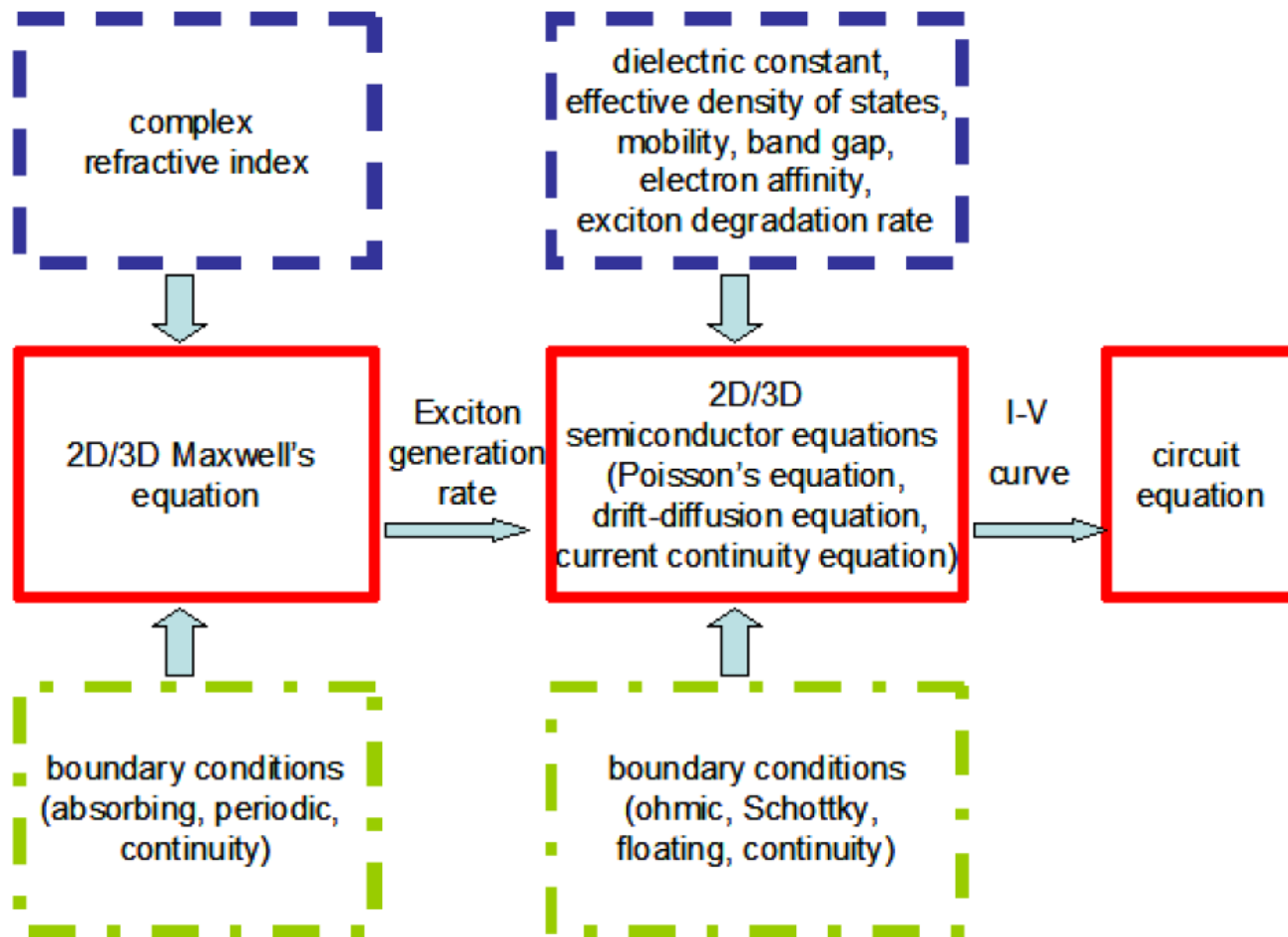


Could electrical properties of OSCs be affected by introducing the metallic nanostructures?



Multiphysics Model (1)

Schematic diagram



Multiphysics Model (2)

Governing equations

frequency dependent permittivity

$$\nabla \times \mathbf{E} = -j\omega\mu_0 \mathbf{H}, \quad \nabla \times \mathbf{H} = j\omega\epsilon(\omega)\mathbf{E}$$

Maxwell's equation

$$G(\mathbf{r}) = \int_{400}^{800} \frac{\lambda}{hc} A(\mathbf{r}, \lambda) d\lambda, \quad A(\mathbf{r}, \lambda) = \omega\epsilon_0 n_r k_i |\mathbf{E}(\mathbf{r})|^2$$

generation rate

$$\nabla \cdot (\epsilon \nabla \phi) = -q(p - n)$$

$$\frac{\partial n}{\partial t} = \frac{1}{q} \nabla \cdot (-q\mu_n n \nabla \phi + qD_n \nabla n) + QG - (1 - Q)R$$

$$\frac{\partial p}{\partial t} = -\frac{1}{q} \nabla \cdot (-q\mu_p p \nabla \phi - qD_p \nabla p) + QG - (1 - Q)R$$

semiconductor equations

electron density *electrostatic potential* *bimolecular recombination rate*
hole density *electrostatic dielectric constant* *exciton dissociation probability*
mobility *Diffusion coefficients*

optical electric field

Generation rate

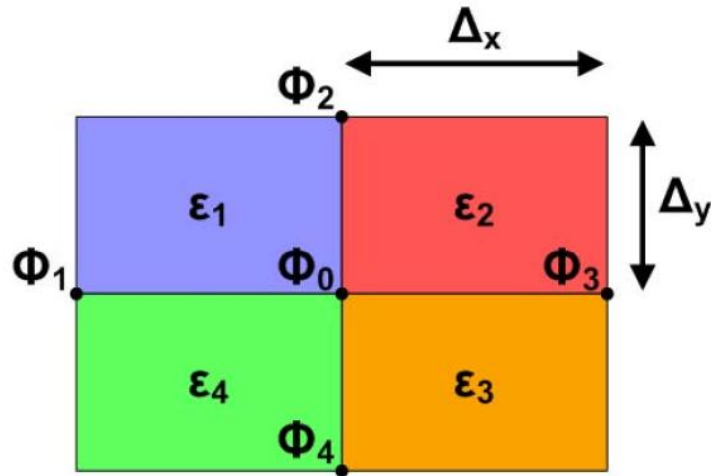


Multiphysics Model (3)

Unified finite difference method

optical properties

spatial step depends on the dielectric wavelength and skin depth of surface plasmons



2D wave equations: TE & TM

$$2 \left(\frac{1}{\Delta_x^2} + \frac{1}{\Delta_y^2} \right) \frac{\Phi_0}{\bar{\epsilon}} - k_0^2 \Phi_0 - \frac{\Phi_1 + \Phi_3}{\bar{\epsilon} \Delta_x^2} - \frac{\Phi_2 + \Phi_4}{\bar{\epsilon} \Delta_y^2} = 0, \quad \Phi = E_z$$

$$2 \left(\frac{1}{\Delta_x^2} + \frac{1}{\Delta_y^2} \right) \frac{\Phi_0}{\bar{\epsilon}} - k_0^2 \Phi_0 - \frac{\epsilon_1^{-1} + \epsilon_4^{-1}}{2\Delta_x^2} \Phi_1 - \frac{\epsilon_2^{-1} + \epsilon_3^{-1}}{2\Delta_x^2} \Phi_3 - \frac{\epsilon_1^{-1} + \epsilon_2^{-1}}{2\Delta_y^2} \Phi_2 - \frac{\epsilon_3^{-1} + \epsilon_4^{-1}}{2\Delta_y^2} \Phi_4 = 0, \quad \Phi = H_z$$

$$\bar{\epsilon} = \begin{cases} \frac{\epsilon_1 + \epsilon_2 + \epsilon_3 + \epsilon_4}{4}, & \Phi = E_z \\ 4(\epsilon_1^{-1} + \epsilon_2^{-1} + \epsilon_3^{-1} + \epsilon_4^{-1})^{-1}, & \Phi = H_z \end{cases}$$

periodic boundary conditions

stretched-coordinate perfectly matched layer



Multiphysics Model (4)

Poisson equation (Gummel's method)

electrical properties

spatial step depends on the Debye length

$$\begin{aligned} & \frac{1}{\Delta_x^2} \epsilon_{i+1/2,j}^d \phi_{i+1,j}^{t+1} + \frac{1}{\Delta_x^2} \epsilon_{i-1/2,j}^d \phi_{i-1,j}^{t+1} + \frac{1}{\Delta_y^2} \epsilon_{i,j+1/2}^d \phi_{i,j+1}^{t+1} + \frac{1}{\Delta_y^2} \epsilon_{i,j-1/2}^d \phi_{i,j-1}^{t+1} \\ & - \left(\epsilon_{i+1/2,j}^d + \epsilon_{i-1/2,j}^d + \epsilon_{i,j+1/2}^d + \epsilon_{i,j-1/2}^d \right) \left(\frac{1}{2\Delta_x^2} + \frac{1}{2\Delta_y^2} \right) \phi_{i,j}^{t+1} - \frac{n_{i,j}^t + p_{i,j}^t}{U_t} \phi_{i,j}^{t+1} \\ & = q(n_{i,j}^t - p_{i,j}^t) - \frac{n_{i,j}^t + p_{i,j}^t}{U_t} \phi_{i,j}^t \end{aligned}$$

drift-diffusion and continuity equations of electron (Scharfetter-Gummel scheme in spatial domain semi-implicit strategy in time domain)

$$\begin{aligned} \frac{n_{i,j}^{t+1} - n_{i,j}^t}{\Delta_t} &= Q_{i,j}^t G_{i,j} - (1 - Q_{i,j}^t) R_{i,j}^t + \frac{D_{i+1/2,j}^n}{\Delta_x^2} B \left(\frac{\phi_{i+1,j}^{t+1} - \phi_{i,j}^{t+1}}{U_t} \right) n_{i+1,j}^{t+1} \\ &+ \frac{D_{i-1/2,j}^n}{\Delta_x^2} B \left(\frac{\phi_{i-1,j}^{t+1} - \phi_{i,j}^{t+1}}{U_t} \right) n_{i-1,j}^{t+1} + \frac{D_{i,j+1/2}^n}{\Delta_y^2} B \left(\frac{\phi_{i,j+1}^{t+1} - \phi_{i,j}^{t+1}}{U_t} \right) n_{i,j+1}^{t+1} \\ &+ \frac{D_{i,j-1/2}^n}{\Delta_y^2} B \left(\frac{\phi_{i,j-1}^{t+1} - \phi_{i,j}^{t+1}}{U_t} \right) n_{i,j-1}^{t+1} - \left[\frac{D_{i+1/2,j}^n}{\Delta_x^2} B \left(\frac{\phi_{i,j}^{t+1} - \phi_{i+1,j}^{t+1}}{U_t} \right) \right. \\ &+ \frac{D_{i-1/2,j}^n}{\Delta_x^2} B \left(\frac{\phi_{i,j}^{t+1} - \phi_{i-1,j}^{t+1}}{U_t} \right) + \frac{D_{i,j+1/2}^n}{\Delta_y^2} B \left(\frac{\phi_{i,j}^{t+1} - \phi_{i,j+1}^{t+1}}{U_t} \right) \\ &\left. + \frac{D_{i,j-1/2}^n}{\Delta_y^2} B \left(\frac{\phi_{i,j}^{t+1} - \phi_{i,j-1}^{t+1}}{U_t} \right) \right] n_{i,j}^{t+1} \end{aligned}$$

scaling unit

cm	$\max \{ \text{DOS} \}^{1/3}$
s	10^{12}
V	1
C	$\frac{1}{1.602 \times 10^{-19}}$
K	$\frac{1}{300}$

Dirichlet and Neumann boundary conditions

time step for stable algorithm

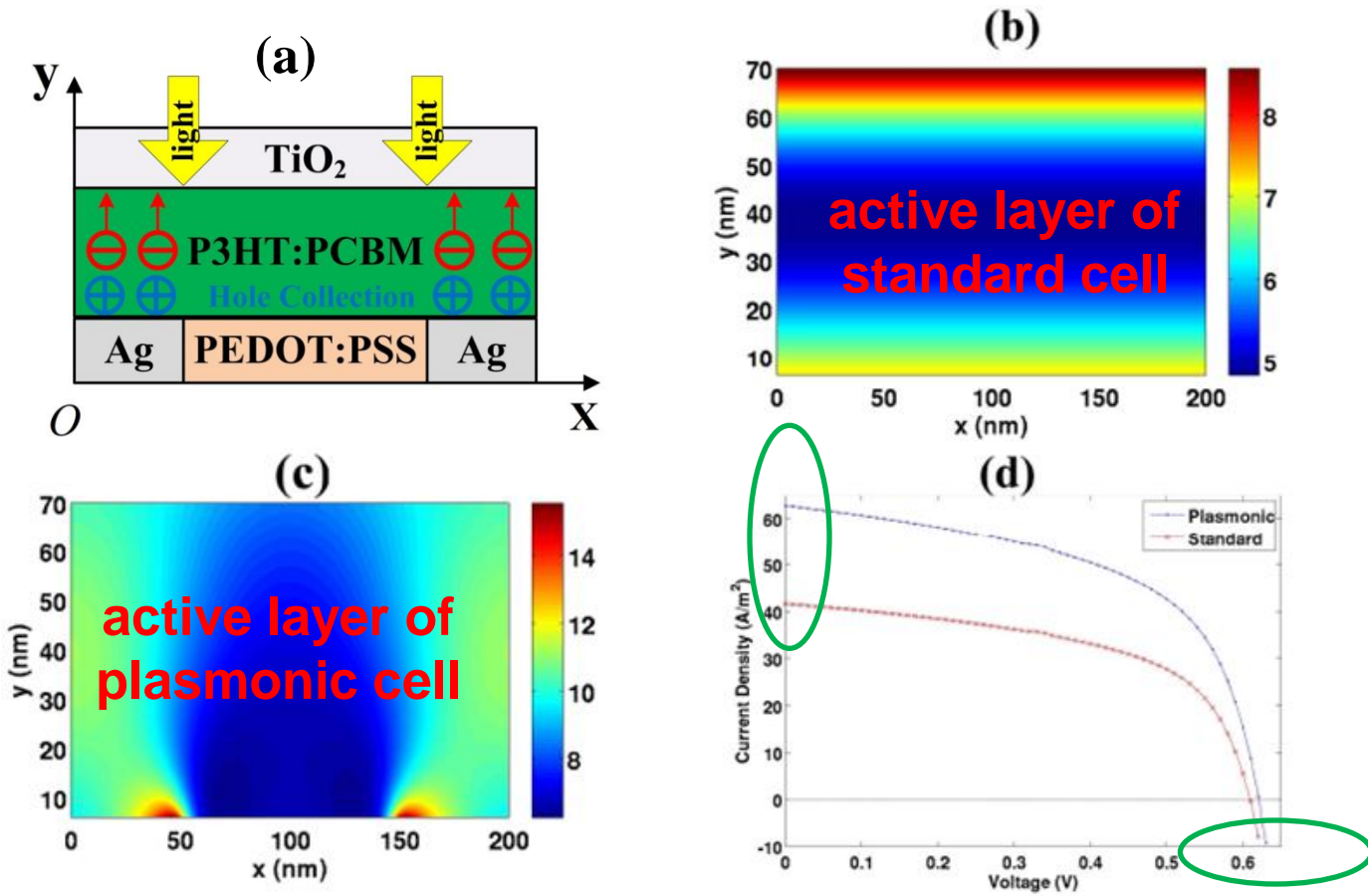
$$\Delta_t < \min \left(\frac{C\epsilon}{\mu_n \cdot n + \mu_p \cdot p} \right)$$



Multiphysics Model (5)

Beyond optical absorption enhancement: facilitating hole collection!

schematic pattern of nanostrip plasmonic cell



Model settings

- active layer thickness 70 nm
- periodicity 200 nm
- PEDOT:PSS width 100 nm
- anode ohmic
- cathode barrier height 0.2 eV
- hole mobility 0.1*electron mobility
- effective band gap 1.1 eV



Multiphysics Model (6)

Characteristic parameters

Plasmonic	J_{sc} (A/m ²)	V_{oc} (V)	MP (W)	FF	PCE (%)
	62.84	0.62	21.47	0.55	2.15
Standard	J_{sc} (A/m ²)	V_{oc} (V)	MP (W)	FF	PCE (%)
	41.67	0.61	14.03	0.55	1.40
Plasmonic	V (V)	J (A/m ²)	\langle Diss \rangle (%)	\langle Rec loss \rangle (%)	
SC	0	62.84	66.96	2.62	
MP	0.48	44.73	58.97	14.55	
OC	0.62	0	55.47	80.88	
Standard	V (V)	J (A/m ²)	\langle Diss \rangle (%)	\langle Rec loss \rangle (%)	
SC	0	41.67	66.96	3.18	
MP	0.47	30.42	59.19	14.93	
OC	0.61	0	55.75	81.91	

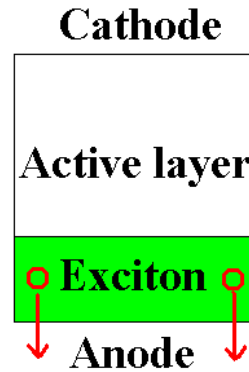
- **reduce recombination loss**
- **increase short-circuit current**
- **improve open-circuit voltage**
- **boost power conversion efficiency**



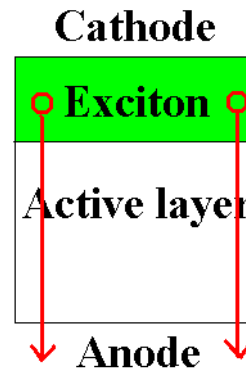
Multiphysics Model (7)

Dummy case for further illustrating physics (hole transport and collection)

$$G_{grating} = \begin{cases} G_c, & d_3 \leq y \leq d_3 + L_g \\ 0, & \text{else} \end{cases}$$

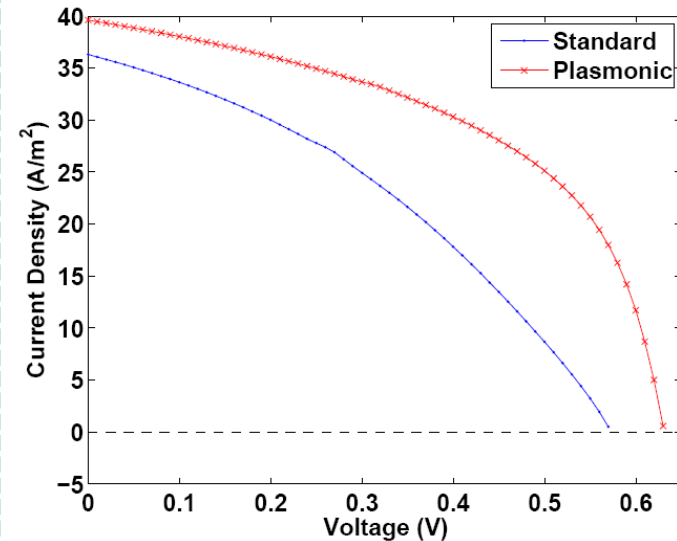


$$G_{planar} = \begin{cases} G_c, & d_3 + d_2 - L_g \leq y \leq d_3 + d_2 \\ 0, & \text{else} \end{cases}$$



hole mobility is set to be two order of magnitude lower than electron mobility

J-V curve

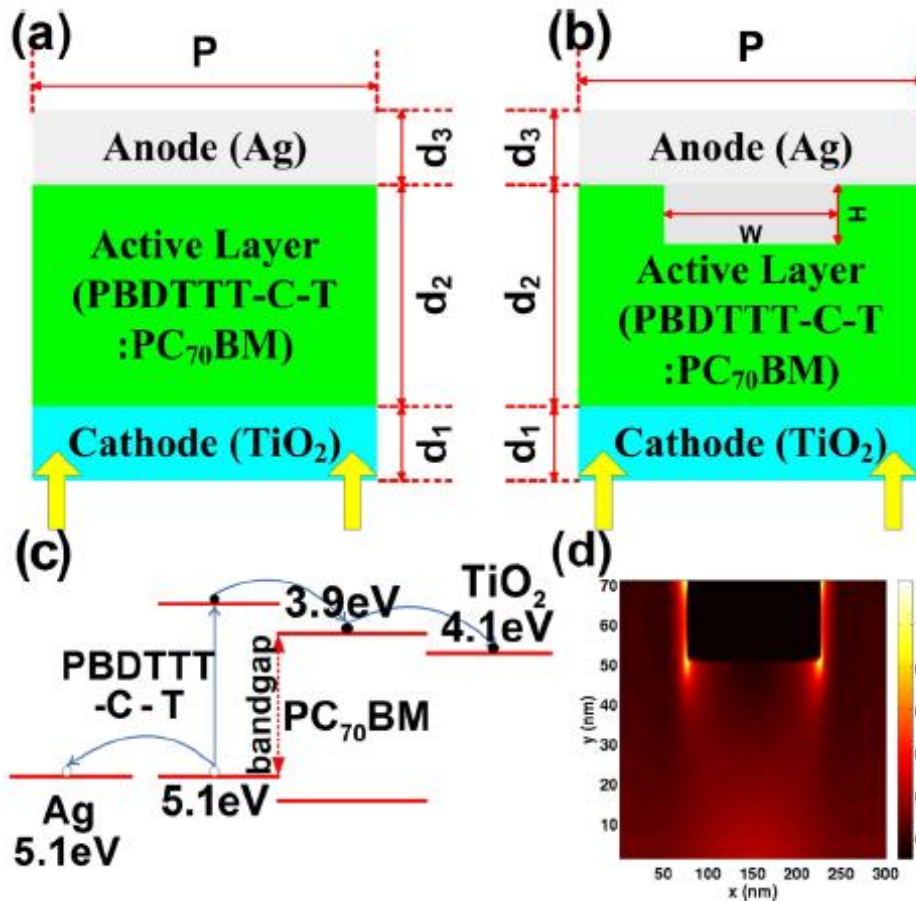


inhomogeneous exciton generation significantly affects fill factor and open-circuit voltage



Multiphysics Model (8)

The nanograting structure v.s. flat standard structure

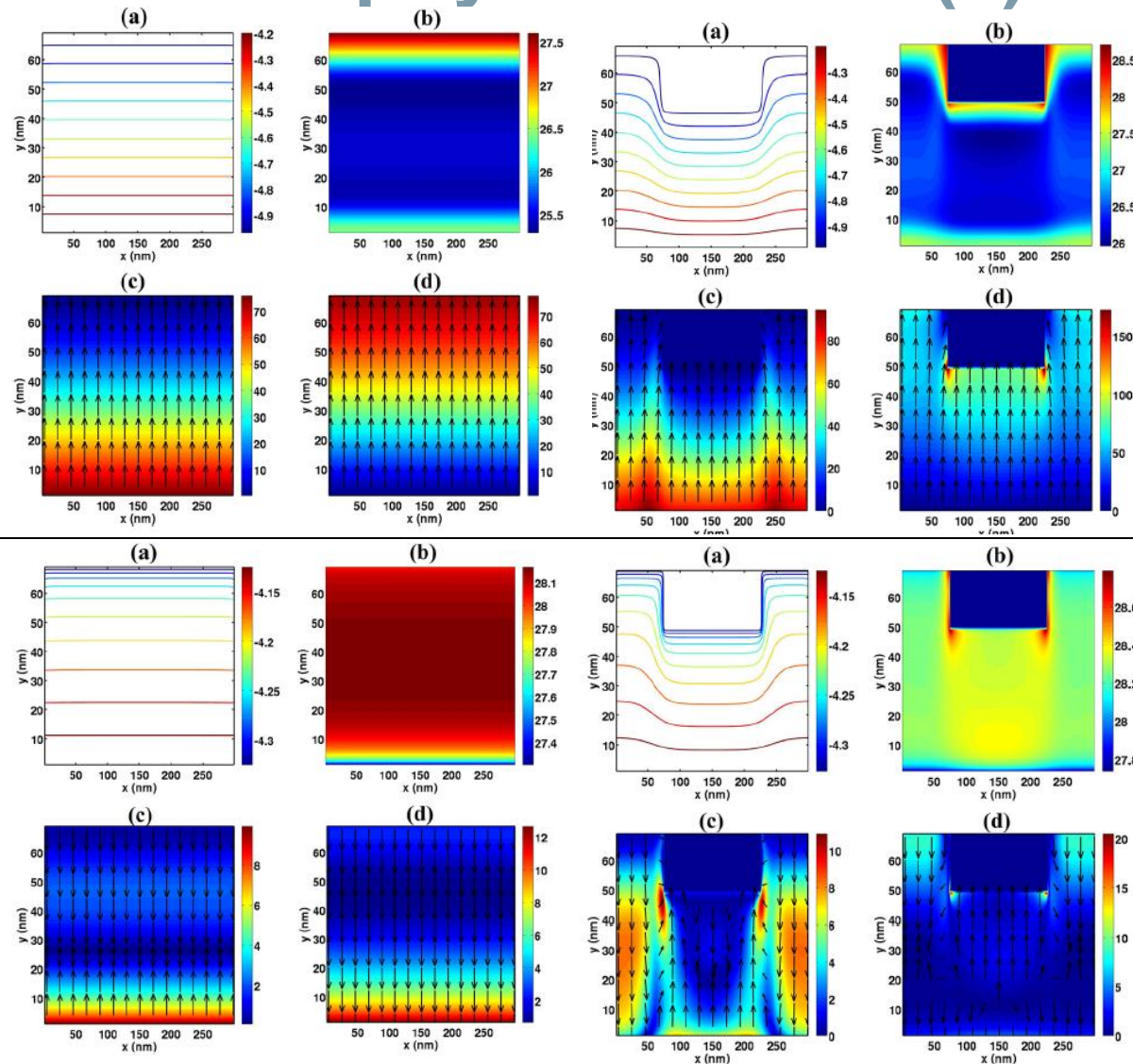


Simulation parameters

E_g	1.2 eV
μ_n	$7.4 \times 10^{-7} \text{ m}^2 / (\text{V} \cdot \text{S})$
μ_p	$7.4 \times 10^{-8} \text{ m}^2 / (\text{V} \cdot \text{S})$
N_c	$2.5 \times 10^{19} \text{ cm}^{-3}$
N_v	$2.5 \times 10^{19} \text{ cm}^{-3}$
ϵ^d	$3.4\epsilon_0 \text{ F/m}$
a	1.12 nm
k_T	$3 \times 10^5 \text{ s}^{-1}$
ψ_b^n	0.2 eV
ψ_b^p	0 eV



Multiphysics Model (9)



short-circuit

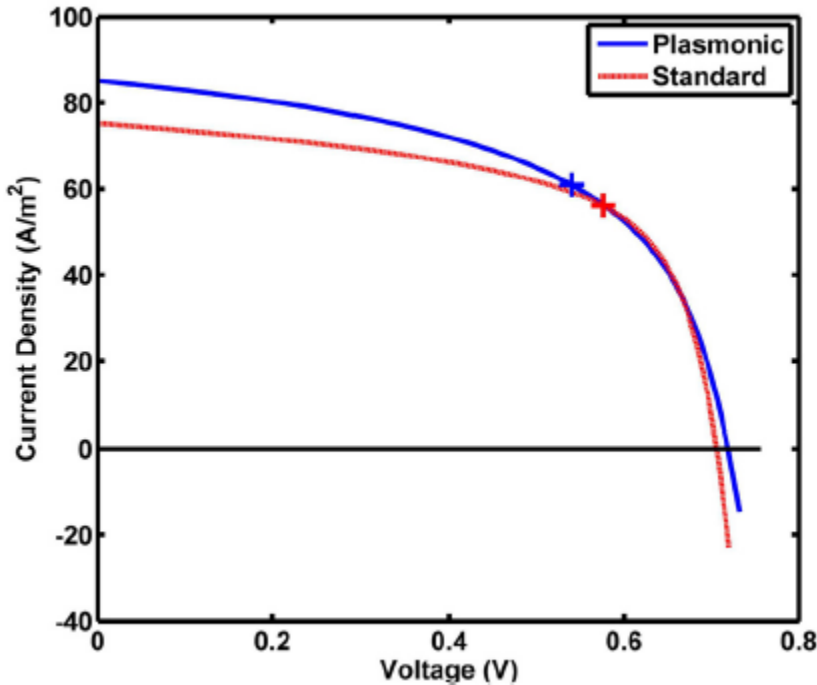
(a) equipotential lines; (b) recombination rate; (c,d) electron and hole current densities.

open-circuit



Multiphysics Model (10)

$$FF = \frac{P_{MAX}}{P_T} = \frac{I_{MP} \cdot V_{MP}}{I_{SC} \cdot V_{OC}}$$



The grating anode induces nonuniform optical absorption and inhomogeneous internal E-field distribution. Thus uneven photocarrier generation and transport are formed in the plasmonic OSC leading to the dropped FF.

TABLE II. The characteristic parameters of the standard and plasmonic OSCs involving short-circuit J_{sc} , open-circuit voltage V_{oc} , MP, FF, and PCE.

	J_{sc} (A/m ²)	V_{oc} (V)	MP (W)	FF (%)	PCE (%)
Standard	75.18	0.706	32.34	60.91	3.23
Plasmonic	85.12	0.719	32.91	53.77	3.29

	SC (Diss)	SC (Rec)	MP (Diss)	MP (Rec)	OC (Diss)	OC (Rec)
Standard (%)	69.83	0.88	62.34	9.19	59.69	82.56
Plasmonic (%)	70.52	2.5	63.38	16.63	59.63	92.75

recombination and exciton dissociation



Acknowledgement

Thanks for your attention!

